NANO LETTERS

pubs.acs.org/NanoLett Letter

Dual-Resonance Nanostructures for Color Downconversion of Colloidal Quantum Emitters

Son Tung Ha,*,⊥ Emmanuel Lassalle,⊥ Xiao Liang, Thi Thu Ha Do, Ian Foo, Sushant Shendre, Emek G. Durmusoglu, Vytautas Valuckas, Sourav Adhikary, Ramon Paniagua-Dominguez, Hilmi Volkan Demir,* and Arseniy I. Kuznetsov*

Cite This: *Nano Lett.* 2023, 23, 11802−11808 Read Online

ACCESS | Metrics & More | Article Recommendations | Supporting Information

ABSTRACT: We present a dual-resonance nanostructure made of a titanium dioxide (TiO_2) subwavelength grating to enhance the color downconversion efficiency of $Cd_xZn_{1-x}Se_yS_{1-y}$ colloidal quantum dots (QDs) emitting at ∼530 nm when excited with a blue light at ∼460 nm. A large mode volume can be created within the QD layer by the hybridization of the grating resonances and waveguide modes, resulting in large absorption and emission enhancements. Particularly, we achieved polarized light emission with a maximum photoluminescence enhancement of ∼140 times at a specific angular direction and a total enhancement of ∼34 times within a 0.55 numerical aperture (NA) of the collecting objective. The enhancement encompasses absorption, Purcell and outcoupling enhancements. We achieved a total absorption of 35% for green QDs with a remarkably thin color conversion layer of ∼400 nm. This work provides a guideline for designing large-volume cavities for absorption/fluorescence enhancement in microLED display, detector, or photovoltaic applications.

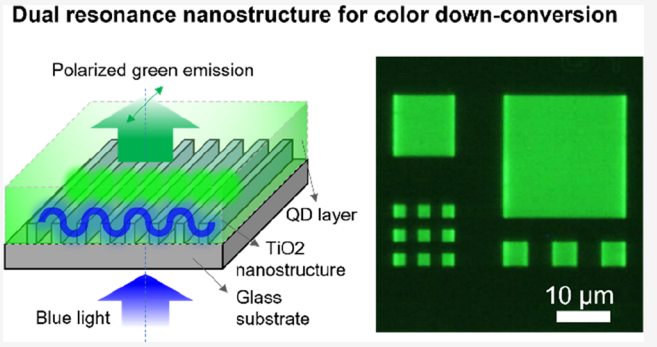

KEYWORDS: *guided mode resonance, titanium dioxide, dielectric nanoantenna, color conversion, colloidal quantum dots, microLED display*

MicroLED is considered a game changer in display technology for emerging applications such as wearable devices, virtual reality (VR), and augmented reality (AR) due to its superior performance in brightness, stability, contrast, and color gamut.[1,2] The main obstacles to this technology are associated with the assembly of millions of microLEDs from different wafers (i.e., for red, green, and blue (RGB)) on the same backplane with zero tolerance for error, the low efficiency of the green microLED, and different driving voltages for RGB channels.[3] To address these challenges, the research and industry communities are now both turning to an alternative approach based on a monolithic blue microLED backplane and a color downconversion layer for green and red using colloidal QDs[4−8] (Figure 1a).

However, this approach also has its own drawbacks such as low color conversion efficiency, crosstalk between pixels, and the patterning of the QDs to sub 10 micron pixels.[9−16] In this regard, a resonant structure can help to solve the aforementioned issues by enhancing the absorption of the QD layer and managing its emission directionality.[17−23] There have been numerous studies in the nanophotonics community to use resonant nanostructures to enhance the fluorescence of emitters based on the Purcell effect.[24−28] These studies have one thing in common: a relatively small mode volume of the resonant structures. This means that only a small amount of QDs within the "hot spots" can couple to the mode and thus be enhanced. A few other approaches have also been studied to enhance color conversion efficiency, such as using a Diffraction Bragg Reflector (DBR),[29] incorporating QDs into InGaN nanorod LEDs,[30] using a mesoporous QD layer,[31] and incorporating high refractive index nanoscatterers (e.g., TiO_2).[8,32−34] However, these approaches have several drawbacks such as low enhancement efficiency, difficulty incorporating QDs into the structures, and requiring modification of a microLED structure (e.g., in InGaN nanorods).

In this work, we propose a resonant nanostructure based on the hybridization of a waveguide mode within the QD layer and a resonant "Bloch mode" originating from the high-index contrast grating made of TiO_2 stripes, as shown in Figure 1b. The resonant structure is designed to have dual resonances at

Received: October 5, 2023
Revised: December 6, 2023
Accepted: December 7, 2023
Published: December 12, 2023

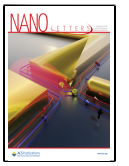

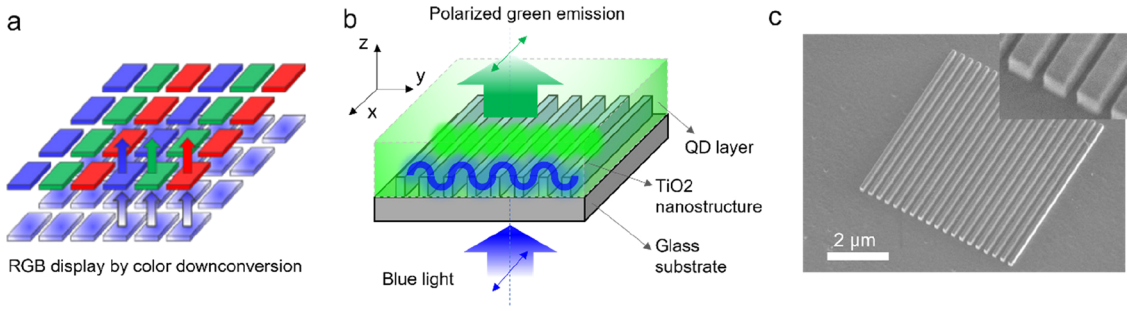

Figure 1. (a) Concept of RGB full-color display by color downconversion using a blue microLED monolithic backplane. (b) Dual-resonance nanoantenna-assisted color downconversion concept used in this work. (c) SEM images of the fabricated TiO_2 nanostructure. The inset shows a "zoomed in" view of an edge of the nanostructure to highlight the quality of the side walls.

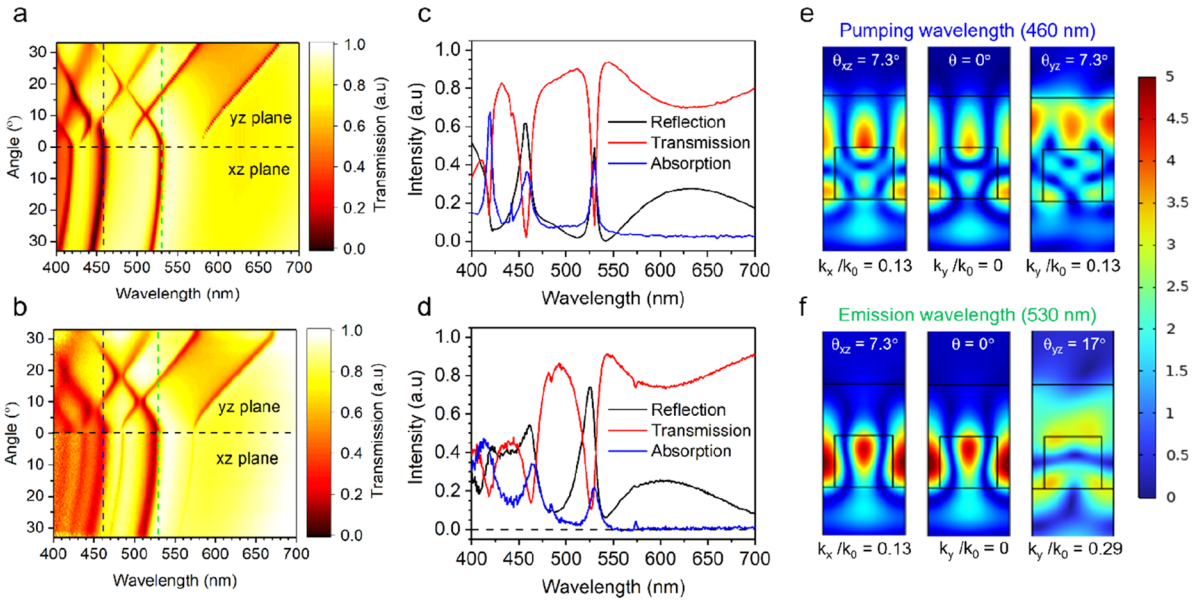

Figure 2. Simulated (a) and measured (b) angle-resolved transmission spectra, for an incident light coming from the glass substrate side with linear polarization along the stripe direction (i.e., along the x axis), in two different planes of incidence: xz plane (bottom halves of the panels) and yz planes (top halves of the panels). Simulated (c) and measured (d) absorption spectra for normally incident excitation (blue) calculated from transmission (red) and reflection (black) spectra. (e) Field distribution at pumping wavelength (i.e., 460 nm) at different k values. (f) Field distribution at the emission wavelength (i.e., 530 nm) at different k values. The k values are defined in air as sin θ, with θ being the angle of incidence.

the blue wavelength (emission peak of microLEDs) and green wavelength (emission peak of green QDs), which can enhance both incoupling (i.e., absorption) and outcoupling (i.e., emission) of polarized light. Most importantly, it has a large mode volume that results in the photoluminescence enhancement of a large number of QDs within the structure.

Design Principle, Fabrication, and Integration of QDs into the Resonant Nanostructure. We chose TiO_2 as the grating stripe material because of its relatively high refractive index and negligible optical loss in the visible region.[35] It is well-known that such high-index contrast grating may support "Bloch mode resonances" (also called "grating resonances") with strong angular response and polarization effects,[36−40] which we will exploit here to mediate the absorption and emission of light by QDs. While the strong angular response offered by such gratings can be an advantage for emission, to make it more directional into a narrow angular cone and enhance the collection efficiency, efficient absorption often needs a rather wide angular response, especially if the source has a nearly isotropic emission (e.g., Lambertian light sources). This can be engineered by carefully controlling another parameter in this design, which is the thickness of the QD layer, in order to support a single waveguide/slab mode band near the wavelength of absorption. In this case, the strong coupling between the slab mode (which is excited by the diffraction from the grating) and the grating/lattice resonance can lead to an avoided crossing, resulting in a "flattening" of the band over a wide angular range.[37] In addition to this, the hybridization of the modes leads to a higher mode overlap with the gain medium, leading to a higher absorption, as will be shown later.

We designed the TiO_2 grating to match two grating resonances (for normal incidence) with the blue (λ = 460 nm) and green (λ = 530 nm) light wavelengths, which are those of interest for absorption and emission, respectively. To do so, the resulting grating has a period Λ = 270 nm, and the stripes have a height H = 200 nm and a width W = 190 nm. The total thickness of the QD layer is designed to be T = 400 nm (i.e., 200 nm additional layer on top of the stripes) to support the first-order transverse electric (TE) slab mode,TE_1,

https://doi.org/10.1021/acs.nanolett.3c03786
Nano Lett. 2023, 23, 11802−11808

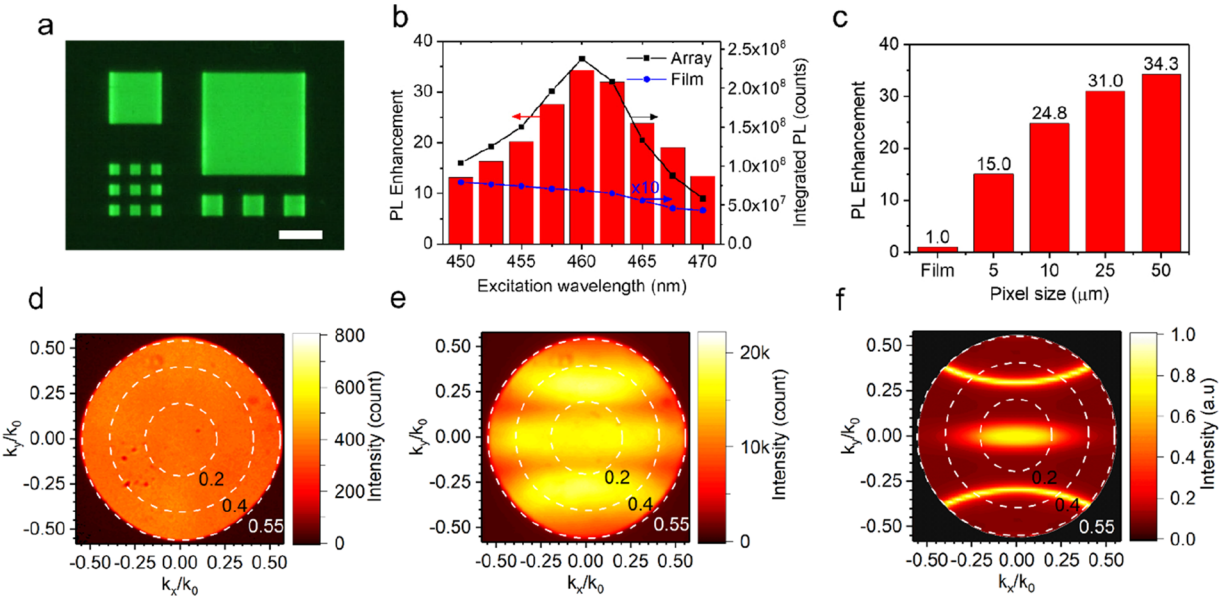

Figure 3. (a) Fluorescence image of nanoantenna enhanced color conversion with different pixel (array) sizes. The scale bar represents 20 μm. (b) Experimental PL enhancement collected with an x-polarized analyzer for different excitation wavelengths for the 50 μm array (red bars), recorded for an unpolarized and normally incident laser excitation. The integrated PL for the nanoantenna array (black dots) and the bare QD film (blue dots) are also shown, for a fixed excitation power and same laser spot size. (c) Experimental PL enhancement collected with an x-polarized analyzer for different pixel sizes when pumping at 460 nm, with all other excitation conditions unchanged. (d, e) Experimental PL BFP images of QDs in a planar film and in a 50 μm pixel, respectively, collected with an x-polarized analyzer. (f) Simulated PL BFP image of the light emission of QDs inside the nanoantennas at 530 nm wavelength linearly polarized along the stripe direction (i.e., x-axis).

around 460 nm. For more details regarding the design, see Section 2, Figures S1−S3 in the Supporting Information. The measured optical constants of TiO_2 and the QDs are given in Section 3, Figures S4 and S5 in the Supporting Information. We then fabricate the TiO_2 grating structures with different array sizes (i.e., 5 × 5, 10 × 10, 20 × 20, and 50 × 50 μm^2) using e-beam lithography and dry etching processes. The detailed nanofabrication parameters can be found in Section 1 in the Supporting Information. Figure 1c shows SEM images of the fabricated 5 × 5 μm^2 grating structure. QDs are then spin-coated onto the fabricated sample. The concentration of QDs and spin-coating speed are controlled to yield an ∼400 nm total thickness of the QDs/TiO_2 grating structure as measured by a profilometer (Section 3, Figure S6 in the Supporting Information).

The optical properties of the samples are characterized using a customized back focal plane microspectrometer (the detailed measurement setup is described in Section 1 in the Supporting Information and elsewhere).[41] Figure 2a,b shows both the simulated and experimentally measured angle-resolved transmission spectra when the system is excited with incident light polarized along the stripes (i.e., x axis) and in two different planes of incidence: the yz plane (top half of the panel) and the xz plane (bottom half of the panel) as defined in Figure 1b. The presence of the resonances can be seen as "dips" in the transmission spectra, as shown in Figure 2c,d (in red), which represent a cut of the angle-resolved spectra at normal incidence (0°). In particular, one can clearly see the two resonance bands at λ = 460 nm and λ = 530 nm. For the former, the avoided crossing between the grating resonance and the slab mode is evident at an incident angle of ∼7.3° in the yz plane (i.e., k_y/k_0 = 0.13), which is a signature of the strong coupling and hybridization between the two modes.[37,38] The strong coupling of these two resonance modes leads to a "flat" band over k_y/k_0 = ±0.13 in the yz plane, which constitutes a total angular range of ∼15° in that plane. For completeness, the simulated angle-resolved transmission spectra of the system when excited with incident light polarized perpendicular to the stripe (i.e., y axis) are shown in Section 4, Figure S7 in the Supporting Information. There, it can be seen that the mode hybridization does not occur, since the design is made to reach the strong coupling condition between modes polarized along the stripes (x axis), i.e. TE Bloch mode and TE waveguide mode (see Section 2 in the Supporting Information). Note that the transmission measured in the xz plane does not present a strong angular dependence since this plane has no periodicity and, therefore, no diffraction, making it less sensitive to the angles of incidence (and similarly for the other polarization, as seen in Section 4, Figure S7 in the Supporting Information). To evidence the importance to finely tune the grating parameters to achieve the strong coupling between different resonances, we show in Section 4, Figure S8 in the Supporting Information an experimental comparison between grating structures having different stripe widths, and how it affects the avoided crossing behavior (i.e., strong coupling).

We then characterize the absorption spectrum of QDs inside the grating structure, as shown in Figure 2c,d (in blue). The absorption spectrum is calculated as $A(\lambda) = 1 - T(\lambda) - R(\lambda)$, where T and R are the transmission and reflection (red and black curves in Figure 2c,d, respectively). The measured angle-resolved reflection and transmission spectra used to calculate the absorption can be found in Section 4, Figure S9 in the Supporting Information. It is noted that there is a slight shift in the absorption peak compared with that of reflection and transmission which may stem from the measurement setup as discussed in detail in Section 1D in the Supporting Information. The result shows that absorption of 35% at 460

https://doi.org/10.1021/acs.nanolett.3c03786
Nano Lett. 2023, 23, 11802−11808

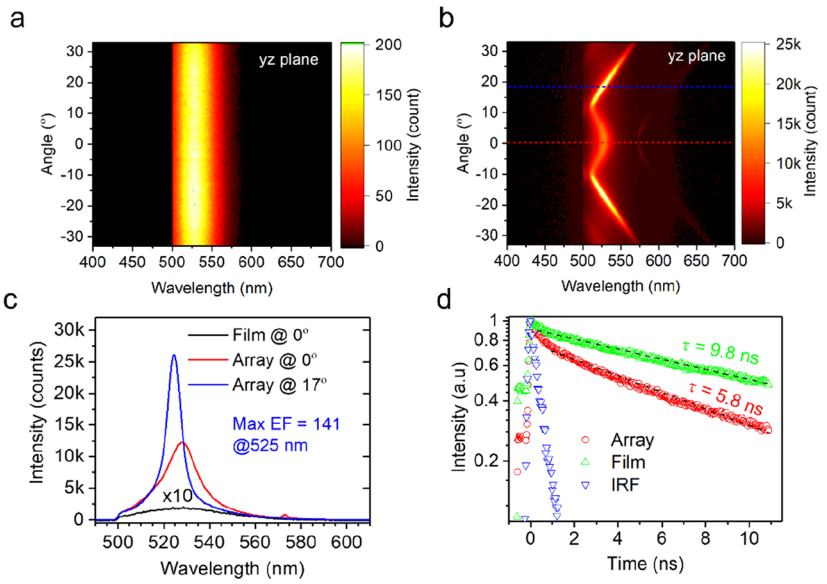

Figure 4. (a, b) Experimental angle-resolved PL spectra in the *yz* plane of QDs in a planar film and the grating structure collected with an *x*-polarized analyzer, respectively. (c) Experimental PL spectra of QDs in the planar film (black line) and the array structure at different emission angles in the *yz* plane (red and blue lines), as shown in (b) (by horizontal red and blue dashed lines). (d) Experimental PL lifetimes of QDs in a planar film (green) and the array structure (red). The instrument response function (IRF) is also shown (blue).

nm excitation is achieved for normal incidence, in excellent agreement with the absorption of 36% obtained from simulations (see Section 5, Figure S10 in the Supporting Information). One of the possible reasons for the moderate absorption is the high reflection (i.e., ∼55%) at the resonance wavelength of 460 nm. It can also be seen that the reabsorption of QD fluorescence may occur at 530 nm due to absorption enhancement caused by the grating resonance at that wavelength. The details of the numerical simulations can be found in Section 1 in the Supporting Information.

Further understanding can be gained by looking at the mode profiles (norm of the electric field) at different points in the resonance bands, as shown in Figure 2e,f. While there is already a good overlapping at $\lambda = 460$ nm between the grating resonance and the QD medium at $k_y/k_0 = 0$ (central panel in Figure 2e, and also in the *xz* plane at $k_x/k_0 = 0.13$, left panel in Figure 2e), which leads to the absorption of 35% observed at normal incidence, the grating resonance clearly gets the nature of a waveguide mode at $k_y/k_0 = 0.13$ (right panel in Figure 2e), which is the result of the strong coupling and mode hybridization. This leads to an even better spatial overlapping between the resonance mode and the QDs layer, as can be seen in the mode profile. Calculations of the absorption of the QDs at this angle $k_y/k_0 = 0.13$ (7.3°), shown in Section 5, Figure S10 in the Supporting Information, reveal that the hybridization of the resonant Bloch mode with the slab mode leads to a maximum of the total absorption of around ∼67% at $\lambda \approx 460$ nm (of which 93% comes from absorption of light in the QDs), in addition to the "flattening" of the band described previously. To achieve such a high value of absorption with a bare QD film, one would need an estimated QD film thickness of ∼5.8 μm (see Section 5 in the Supporting Information).

Regarding the band at $\lambda \approx 530$ nm ($k_y/k_0 = 0$), exploited to enhance the emission by the QDs, we also show the corresponding mode profile in Figure 2f (middle panel). One can see that the electric field still extends outside of the TiO_2 stripes, even if the overlap with the gain medium is less than that of the resonance at 460 nm. Modal analysis of the electric and magnetic field components reveals that this resonance at $\lambda = 530$ nm is essentially an in-plane electric dipole mode in nature (along the stripe direction, i.e. along the *x*-axis). We also note that for the other polarization, there is no resonance at $\lambda = 530$ nm (see Section 4, Figure S7 in the Supporting Information). Therefore, one can expect an enhancement of linearly polarized light emission along the *x*-axis at the QD emission wavelength, as we will see hereafter.

Color Downconversion Performance. Figure 3a shows the wide-field PL images of the fabricated sample. The green pixels correspond to the area where the grating structures are present, while the "dark" area is the bare quantum dot film. It can be seen that the nanoantennas have significantly enhanced the PL of QDs down to a pixel size as small as 5×5 μm^2. To investigate the effect of the excitation wavelength on the PL enhancement, a tunable laser (SuperK, NKT Photonics equipped with SuperK Select optical filter) with a 40% degree of polarization along *x* is used to excite the QDs at normal incidence. The total PL signals are collected using a 50× objective (0.55 NA) with a linear analyzer along the stripe direction (i.e., along the *x* axis). The total PL enhancement is calculated by comparing the PL of QDs in the 50×50 μm^2 nanoantenna pixel with that of the bare QD film for each excitation condition, as shown in Figure 3b. As expected, the maximum total PL enhancement of ∼34 is achieved when the excitation wavelength is set at 460 nm, corresponding to the designed resonance wavelength. By comparing the total PL enhancement when pumping at resonance wavelength (i.e., 460 nm) and nonresonance wavelength (i.e., 470 nm), we can estimate the absorption enhancement of ∼3.5 times. The rest of the enhancement is attributed to the Purcell effect and outcoupling enhancement of the emission at the second resonance (i.e., 530 nm), which will be further demonstrated below. Similar experiments were done for different pixel sizes as shown in Figure 3c. It can be seen that as the pixel size decreases from 50 to 5 μm, the total PL enhancement drops from ∼34 to about 15. This can be explained by the fact that the resonances are designed on the basis of lattice resonances,

https://doi.org/10.1021/acs.nanolett.3c03786
Nano Lett. 2023, 23, 11802−11808

which strongly depend on the array size. Nevertheless, a reasonable enhancement can be achieved with a pixel size as small as 5 × 5 μm^2, which is enough for most VR and AR applications.

Regarding the emission, Figures 3d,e shows the BFP images of the QD emission in a bare film and in the 50 μm pixel, respectively, for a linear polarization along the x-axis. It can be seen that, in the nanoantenna sample, the emission of QDs is concentrated in three lobes in the radiation pattern (Figure 3e). This observation agrees well with the simulated emission pattern, as shown in Figure 3f. The narrower emission band in the simulation compared to the experiment is because the calculation is for a single wavelength at 530 nm rather than the whole emission spectrum. In the radiation pattern, the central lobe is coming from the coupling to the grating resonance at normal incidence which is identified as an electric dipole resonance along the x-axis, as discussed in Figure 2a,b, while the two side lobes are coming from the coupling to another grating resonance that can be seen at around 16.7° in the yz plane (i.e., $k_y/k_0 = 0.29$ and $k_x/k_0 = 0$) in Figure 2a,b. The simulation results for full radiation patterns of both linear polarizations along the x- and y-axes can be found in Figure S11 in the Supporting Information. As expected, there is no central lobe for linearly polarized light along the y-axis, since there is no resonance at normal incidence, while two side lobes can be seen, corresponding to the coupling to another grating resonance that can be observed at around 21.7° in the yz plane (i.e., $k_y/k_0 = 0.37$ and $k_x/k_0 = 0$) in Section 4, Figure S7 in the Supporting Information. Setting apart the side lobes, the nanoantenna therefore enhances linearly polarized light emission along the x-axis.

To further characterize the enhancement of QD emission in the nanoantenna sample, angle-resolved spectroscopy measurements are performed. Figure 4a,b shows the spectrally resolved PL emission in the yz plane of the QDs in a bare film and in the nanoantenna structure, respectively. It can be seen again that the PL of QDs couples to two different resonances of the nanoantennas. The mode profiles of the two modes (i.e., $k_y/k_0 = 0$ and $k_y/k_0 = 0.29$) were previously shown in Figure 2f, middle and right panels, respectively. Figure 4c shows the emission spectra of QDs coupled to these two modes in comparison to that of the bare film of QDs. It can be seen that a maximum PL enhancement of 141 times at 525 nm for the emission angle of ∼17° in the yz plane (i.e., $k_y/k_0 = 0.29$ and $k_x/k_0 = 0$) is achieved. PL lifetime measurements are also done at this particular wavelength (i.e., 525 nm), as shown in Figure 4d. It can be seen that the PL lifetime of QDs decreases from 9.8 ns for the bare film to 5.8 ns for the grating structure, indicating a lifetime reduction (i.e., Purcell enhancement).

In conclusion, we present a concept of a dual-resonance nanostructure with a large mode volume to enhance both the absorption and the polarized light emission of quantum emitters applicable for color downconversion in display technology. The hybridization of a grating resonance in the high index contrast grating and a waveguide mode within the QD layer is responsible for better spatial mode overlapping and an angularly "flat-band" resonance at the excitation wavelength over an angular range of 15°. Thus, we report experimentally an absorption of 35% at 460 nm for green QDs for an excitation at normal incidence, which is remarkably high for such a thin color conversion film of ∼400 nm (inclusive of the TiO_2 grating layer), while in simulations the total absorption ranges from 36% (at normal incidence) to up to 67% within the angular range of 15°. Moreover, we obtain a highly linear polarized light emission (along the stripes) without the need of filtering, with a total PL enhancement of 34.3 times within the field of view of ±33° and a maximum enhancement of 141 times at 525 nm wavelength and viewing angle of 17° (i.e., $k_y/k_0 = 0.29$) in comparison to a bare QD film. Our work suggests that high-index dielectric nanoantennas can be used to create efficient resonant structures suitable for color conversion in practical applications such as microLED displays and sensitizer-assisted detectors.

■ ASSOCIATED CONTENT

Supporting Information

The Supporting Information is available free of charge at https://pubs.acs.org/doi/10.1021/acs.nanolett.3c03786.

Materials (QD synthesis and film preparation) and methods (nanofabrication, optical characterizations and simulation), design principles of the resonance nanostructures, QD optical properties, film morphology, additional angle-resolved transmission/reflection spectra of the samples, and absorption calculations of the QDs inside the nanostructures (PDF)

■ AUTHOR INFORMATION

Corresponding Authors

Son Tung Ha − *Institute of Materials Research and Engineering (IMRE), Agency for Science Technology and Research (A*STAR), Singapore 138634, Republic of Singapore;* orcid.org/0000-0002-5475-8365; Email: ha_son_tung@imre.a-star.edu.sg

Hilmi Volkan Demir − *LUMINOUS! Center of Excellence for Semiconductor Lighting and Displays, The Photonics Institute, School of Electrical and Electronic Engineering, Nanyang Technological University, Singapore 639798, Singapore; Division of Physics and Applied Physics, School of Physical and Mathematical Sciences, Nanyang Technological University, Singapore 637371, Singapore; UNAM—Institute of Materials Science and Nanotechnology, The National Nanotechnology Research Center, Department of Electrical and Electronics Engineering, Department of Physics, Bilkent University, Ankara 06800, Turkey;* orcid.org/0000-0003-1793-112X; Email: hvdemir@ntu.edu.sg

Arseniy I. Kuznetsov − *Institute of Materials Research and Engineering (IMRE), Agency for Science Technology and Research (A*STAR), Singapore 138634, Republic of Singapore;* orcid.org/0000-0002-7622-8939; Email: arseniy_kuznetsov@imre.a-star.edu.sg

Authors

Emmanuel Lassalle − *Institute of Materials Research and Engineering (IMRE), Agency for Science Technology and Research (A*STAR), Singapore 138634, Republic of Singapore;* orcid.org/0000-0002-0098-5159

Xiao Liang − *LUMINOUS! Center of Excellence for Semiconductor Lighting and Displays, The Photonics Institute, School of Electrical and Electronic Engineering, Nanyang Technological University, Singapore 639798, Singapore*

Thi Thu Ha Do − *Institute of Materials Research and Engineering (IMRE), Agency for Science Technology and Research (A*STAR), Singapore 138634, Republic of Singapore*

Ian Foo − *Institute of Materials Research and Engineering (IMRE), Agency for Science Technology and Research (A*STAR), Singapore 138634, Republic of Singapore*

Sushant Shendre − *LUMINOUS! Center of Excellence for Semiconductor Lighting and Displays, The Photonics Institute, School of Electrical and Electronic Engineering, Nanyang Technological University, Singapore 639798, Singapore*

Emek G. Durmusoglu − *LUMINOUS! Center of Excellence for Semiconductor Lighting and Displays, The Photonics Institute, School of Electrical and Electronic Engineering, Nanyang Technological University, Singapore 639798, Singapore; Division of Physics and Applied Physics, School of Physical and Mathematical Sciences, Nanyang Technological University, Singapore 637371, Singapore;* orcid.org/0000-0001-6840-8342

Vytautas Valuckas − *Institute of Materials Research and Engineering (IMRE), Agency for Science Technology and Research (A*STAR), Singapore 138634, Republic of Singapore*

Sourav Adhikary − *Institute of Materials Research and Engineering (IMRE), Agency for Science Technology and Research (A*STAR), Singapore 138634, Republic of Singapore*

Ramon Paniagua-Dominguez − *Institute of Materials Research and Engineering (IMRE), Agency for Science Technology and Research (A*STAR), Singapore 138634, Republic of Singapore;* orcid.org/0000-0001-7836-681X

Complete contact information is available at: https://pubs.acs.org/10.1021/acs.nanolett.3c03786

Author Contributions

[⊥]S.T.H. and E.L. contributed equally.

Author Contributions

S.T.H., R.P.-D., and A.I.K. initiated the idea of the project. R.P.-D. proposed the conceptual design, I.F. did the initial design and simulations, and E.L. finalized the design and did all other simulations, supervised by R.P.-D. S.T.H. and T.T.H.D. fabricated the TiO_2 nanostructures and did all back focal plane measurements. V.V. and S.A. deposited TiO_2 films. X.L., S.S., E.G.D., and H.V.D. synthesized and characterized QDs and prepared QD films. S.T.H., H.V.D., and A.I.K. supervised the project. The manuscript was written through contributions of all authors. All authors have given approval to the final version of the manuscript.

Notes

The authors declare no competing financial interest.

■ ACKNOWLEDGMENTS

The authors acknowledges funding support from Singapore MTC-Programmatic Grant No. M21J9b0085. S.T.H. also acknowledges support under the Singapore AME Young Individual Research Grant No. A2084c0177.

■ REFERENCES

(1) Anwar, A. R.; Sajjad, M. T.; Johar, M. A.; Hernández-Gutiérrez, C. A.; Usman, M.; Łepkowski, S. P. Recent Progress in Micro-LED-Based Display Technologies. *Laser Photonics Rev.* **2022**, *16* (6), No. 2100427.

(2) Liu, Z.; Lin, C.-H.; Hyun, B.-R.; Sher, C.-W.; Lv, Z.; Luo, B.; Jiang, F.; Wu, T.; Ho, C.-H.; Kuo, H.-C.; He, J.-H. Micro-Light-Emitting Diodes with Quantum Dots in Display Technology. *Light Sci. Appl.* **2020**, *9* (1), 83.

(3) Zhou, X.; Tian, P.; Sher, C.-W.; Wu, J.; Liu, H.; Liu, R.; Kuo, H.-C. Growth, Transfer Printing and Colour Conversion Techniques towards Full-Colour Micro-LED Display. *Prog. Quantum Electron.* **2020**, *71*, No. 100263.

(4) Klimov, V. I.; Mikhailovsky, A. A.; Xu, S.; Malko, A.; Hollingsworth, J. A.; Leatherdale, C. A.; Eisler, H.-J.; Bawendi, M. G. Optical Gain and Stimulated Emission in Nanocrystal Quantum Dots. *Science* **2000**, *290* (5490), 314−317.

(5) Yang, J.; Choi, M. K.; Yang, U. J.; Kim, S. Y.; Kim, Y. S.; Kim, J. H.; Kim, D.-H.; Hyeon, T. Toward Full-Color Electroluminescent Quantum Dot Displays. *Nano Lett.* **2021**, *21* (1), 26−33.

(6) Dai, X.; Zhang, Z.; Jin, Y.; Niu, Y.; Cao, H.; Liang, X.; Chen, L.; Wang, J.; Peng, X. Solution-Processed, High-Performance Light-Emitting Diodes Based on Quantum Dots. *Nature* **2014**, *515* (7525), 96−99.

(7) Ko, Y.-H.; Jalalah, M.; Lee, S.-J.; Park, J.-G. Super Ultra-High Resolution Liquid-Crystal-Display Using Perovskite Quantum-Dot Functional Color-Filters. *Sci. Rep.* **2018**, *8* (1), 12881.

(8) Li, Z.-T.; Li, J.-X.; Li, J.-S.; Deng, Z.-H.; Deng, Y.-H.; Tang, Y. Scattering Effect on Optical Performance of Quantum Dot White Light-Emitting Diodes Incorporating SiO_2Nanoparticles. *IEEE J. Quantum Electron.* **2020**, *56* (3), 1−9.

(9) Kim, W. H.; Jang, Y. J.; Kim, J.-Y.; Han, M.; Kang, M.; Yang, K.; Ryou, J.-H.; Kwon, M.-K. High-Performance Color-Converted Full-Color Micro-LED Arrays. *Appl. Sci.* **2020**, *10* (6), 2112.

(10) Chu, S.-Y.; Wang, H.-Y.; Lee, C.-T.; Lee, H.-Y.; Laing, K.-L.; Kuo, W.-H.; Fang, Y.-H.; Lin, C.-C. Improved Color Purity of Monolithic Full Color Micro-LEDs Using Distributed Bragg Reflector and Blue Light Absorption Material. *Coatings* **2020**, *10* (5), 436.

(11) Xuan, T.; Shi, S.; Wang, L.; Kuo, H.-C.; Xie, R.-J. Inkjet-Printed Quantum Dot Color Conversion Films for High-Resolution and Full-Color Micro Light-Emitting Diode Displays. *J. Phys. Chem. Lett.* **2020**, *11* (13), 5184−5191.

(12) Guilhabert, B.; Elfström, D.; Kuehne, A. J. C.; Massoubre, D.; Zhang, H. X.; Jin, S. R.; Mackintosh, A. R.; Gu, E.; Pethrick, R. A.; Dawson, M. D. Integration by Self-Aligned Writing of Nanocrystal/Epoxy Composites on InGaN Micro-Pixelated Light-Emitting Diodes. *Opt. Express* **2008**, *16* (23), 18933−18941.

(13) Chen, G.-S.; Wei, B.-Y.; Lee, C.-T.; Lee, H.-Y. Monolithic Red/Green/Blue Micro-LEDs With HBR and DBR Structures. *IEEE Photonics Technol. Lett.* **2018**, *30* (3), 262−265.

(14) Srivastava, S.; Lee, K. E.; Fitzgerald, E. A.; Pennycook, S. J.; Gradečak, S. Freestanding High-Resolution Quantum Dot Color Converters with Small Pixel Sizes. *ACS Appl. Mater. Interfaces* **2022**, *14* (43), 48995−49002.

(15) Hyun, B.-R.; Sher, C.-W.; Chang, Y.-W.; Lin, Y.; Liu, Z.; Kuo, H.-C. Dual Role of Quantum Dots as Color Conversion Layer and Suppression of Input Light for Full-Color Micro-LED Displays. *J. Phys. Chem. Lett.* **2021**, *12* (29), 6946−6954.

(16) Liu, C.-Y.; Chen, T.-P.; Kao, T. S.; Huang, J.-K.; Kuo, H.-C.; Chen, Y.-F.; Chang, C.-Y. Color-Conversion Efficiency Enhancement of Quantum Dots via Selective Area Nano-Rods Light-Emitting Diodes. *Opt. Express* **2016**, *24* (17), 19978−19987.

(17) Han, H.-V.; Lin, H.-Y.; Lin, C.-C.; Chong, W.-C.; Li, J.-R.; Chen, K.-J.; Yu, P.; Chen, T.-M.; Chen, H.-M.; Lau, K.-M.; Kuo, H.-C. Resonant-Enhanced Full-Color Emission of Quantum-Dot-Based Micro LED Display Technology. *Opt. Express* **2015**, *23* (25), 32504−32515.

(18) Vaskin, A.; Kolkowski, R.; Koenderink, A. F.; Staude, I. Light-Emitting Metasurfaces. *Nanophotonics* **2019**, *8* (7), 1151−1198.

(19) Liu, S.; Vaskin, A.; Addamane, S.; Leung, B.; Tsai, M.-C.; Yang, Y.; Vabishchevich, P. P.; Keeler, G. A.; Wang, G.; He, X.; Kim, Y.; Hartmann, N. F.; Htoon, H.; Doorn, S. K.; Zilk, M.; Pertsch, T.; Balakrishnan, G.; Sinclair, M. B.; Staude, I.; Brener, I. Light-Emitting Metasurfaces: Simultaneous Control of Spontaneous Emission and Far-Field Radiation. *Nano Lett.* **2018**, *18* (11), 6906−6914.

(20) Dong, Z.; Gorelik, S.; Paniagua-Dominguez, R.; Yik, J.; Ho, J.; Tjiptoharsono, F.; Lassalle, E.; Rezaei, S. D.; Neo, D. C. J.; Bai, P.; Kuznetsov, A. I.; Yang, J. K. W. Silicon Nanoantenna Mix Arrays for a

Trifecta of Quantum Emitter Enhancements. *Nano Lett.* **2021**, *21* (11), 4853−4860.
(21) Xiong, Y.; Huang, Q.; Canady, T. D.; Barya, P.; Liu, S.; Arogundade, O. H.; Race, C. M.; Che, C.; Wang, X.; Zhou, L.; Wang, X.; Kohli, M.; Smith, A. M.; Cunningham, B. T. Photonic crystal enhanced fluorescence emission and blinking suppression for single quantum dot digital resolution biosensing. *Nat. Commun.* **2022**, *13*, 4647.
(22) Feng, Z.; Shi, T.; Geng, G.; Li, J.; Deng, Z. L.; Kivshar, Y.; Li, X. Dual-band polarized upconversion photoluminescence enhanced by resonant dielectric metasurfaces. *eLight* **2023**, *3*, No. 21.
(23) Liu, H. L.; Xu, J.; Wang, H.; Liu, Y.; Ruan, Q.; Wu, Y.; Liu, X.; Yang, Y. K. W. Tunable Resonator-Upconverted Emission (TRUE) Color Printing and Applications in Optical Security. *Adv. Mater.* **2019**, *31* (15), No. 1807900.
(24) Dmitriev, P. A.; Lassalle, E.; Ding, L.; Pan, Z.; Neo, D. C. J.; Valuckas, V.; Paniagua-Dominguez, R.; Yang, J. K. W.; Demir, H. V.; Kuznetsov, A. I. Hybrid Dielectric-Plasmonic Nanoantenna with Multiresonances for Subwavelength Photon Sources. *ACS Photonics* **2023**, *10* (3), 582−594.
(25) Marquier, F.; Sauvan, C.; Greffet, J.-J. Revisiting Quantum Optics with Surface Plasmons and Plasmonic Resonators. *ACS Photonics* **2017**, *4* (9), 2091−2101.
(26) Akselrod, G. M.; Argyropoulos, C.; Hoang, T. B.; Ciracì, C.; Fang, C.; Huang, J.; Smith, D. R.; Mikkelsen, M. H. Probing the Mechanisms of Large Purcell Enhancement in Plasmonic Nanoantennas. *Nat. Photonics* **2014**, *8* (11), 835−840.
(27) Kühn, S.; Håkanson, U.; Rogobete, L.; Sandoghdar, V. Enhancement of Single-Molecule Fluorescence Using a Gold Nanoparticle as an Optical Nanoantenna. *Phys. Rev. Lett.* **2006**, *97* (1), No. 017402.
(28) Anger, P.; Bharadwaj, P.; Novotny, L. Enhancement and Quenching of Single-Molecule Fluorescence. *Phys. Rev. Lett.* **2006**, *96* (11), No. 113002.
(29) Joo, W.-J.; Kyoung, J.; Esfandyarpour, M.; Lee, S.-H.; Koo, H.; Song, S.; Kwon, Y.-N.; Song, S. H.; Bae, J. C.; Jo, A.; Kwon, M.-J.; Han, S. H.; Kim, S.-H.; Hwang, S.; Brongersma, M. L. Metasurface-Driven OLED Displays beyond 10,000 Pixels per Inch. *Science* **2020**, *370* (6515), 459−463.
(30) Lee, Y.-J.; Lee, C.-J.; Cheng, C.-M. Enhancing the Conversion Efficiency of Red Emission by Spin-Coating CdSe Quantum Dots on the Green Nanorod Light-Emitting Diode. *Opt. Express* **2010**, *18* (104), A554−A561.
(31) Li, J.; Tang, Y.; Li, Z.; Ding, X.; Yu, B.; Lin, L. Largely Enhancing Luminous Efficacy, Color-Conversion Efficiency, and Stability for Quantum-Dot White LEDs Using the Two-Dimensional Hexagonal Pore Structure of SBA-15 Mesoporous Particles. *ACS Appl. Mater. Interfaces* **2019**, *11* (20), 18808−18816.
(32) Tang, Y.; Li, Z.; Li, Z.-T.; Li, J.-S.; Yu, S.-D.; Rao, L.-S. Enhancement of Luminous Efficiency and Uniformity of CCT for Quantum Dot-Converted LEDs by Incorporating With ZnO Nanoparticles. *IEEE Trans. Electron Devices* **2018**, *65* (1), 158−164.
(33) Li, J.-S.; Tang, Y.; Li, Z.-T.; Li, Z.; Ding, X.-R.; Rao, L.-S. Investigation of the Emission Spectral Properties of Carbon Dots in Packaged LEDs Using TiO2 Nanoparticles. *IEEE J. Sel. Top. Quantum Electron.* **2017**, *23* (5), 1−7.
(34) Xie, B.; Liu, H.; Hu, R.; Wang, C.; Hao, J.; Wang, K.; Luo, X. Targeting Cooling for Quantum Dots in White QDs-LEDs by Hexagonal Boron Nitride Platelets with Electrostatic Bonding. *Adv. Funct. Mater.* **2018**, *28* (30), No. 1801407.
(35) Wu, M.; Ha, S. T.; Shendre, S.; Durmusoglu, E. G.; Koh, W.-K.; Abujetas, D. R.; Sánchez-Gil, J. A.; Paniagua-Domínguez, R.; Demir, H. V.; Kuznetsov, A. I. Room-Temperature Lasing in Colloidal Nanoplatelets via Mie-Resonant Bound States in the Continuum. *Nano Lett.* **2020**, *20* (8), 6005−6011.
(36) Lalanne, P.; Hugonin, J. P.; Chavel, P. Optical Properties of Deep Lamellar Gratings: A Coupled Bloch-Mode Insight. *J. Light. Technol.* **2006**, *24* (6), 2442−2449.
(37) Lu, L.; Le-Van, Q.; Ferrier, L.; Drouard, E.; Seassal, C.; Nguyen, H. S. Engineering a Light−Matter Strong Coupling Regime in Perovskite-Based Plasmonic Metasurface: Quasi-Bound State in the Continuum and Exceptional Points. *Photonics Res.* **2020**, *8* (12), A91−A100.
(38) Bykov, D. A.; Bezus, E. A.; Doskolovich, L. L. Coupled-Wave Formalism for Bound States in the Continuum in Guided-Mode Resonant Gratings. *Phys. Rev. A* **2019**, *99* (6), No. 063805.
(39) Ha, S. T.; Paniagua-Domínguez, R.; Kuznetsov, A. I. Room-Temperature Multi-Beam, Multi-Wavelength Bound States in the Continuum Laser. *Adv. Opt. Mater.* **2022**, *10* (19), No. 2200753.
(40) Azzam, S. I.; Shalaev, V. M.; Boltasseva, A.; Kildishev, A. V. Formation of Bound States in the Continuum in Hybrid Plasmonic-Photonic Systems. *Phys. Rev. Lett.* **2018**, *121* (25), No. 253901.
(41) Ha, S. T.; Fu, Y. H.; Emani, N. K.; Pan, Z.; Bakker, R. M.; Paniagua-Domínguez, R.; Kuznetsov, A. I. Directional Lasing in Resonant Semiconductor Nanoantenna Arrays. *Nat. Nanotechnol.* **2018**, *13* (11), 1042−1047.

https://doi.org/10.1021/acs.nanolett.3c03786
Nano Lett. 2023, 23, 11802−11808